J Mater Sci (2007) 42:215–220
DOI 10.1007/s10853-006-1054-z

Compositional dependence of some physical properties of $ZnO–PbO–P_2O_5$ glasses

H. Tichá · J. Schwarz · L. Tichý

Received: 29 November 2005 / Accepted: 10 January 2006 / Published online: 11 November 2006

Abstract Six glasses of the chemical composition $10ZnO–xPbO–(90–x)\ P_2O_5$ were prepared. With an increase in PbO content a non-monotonous step like increase in the density, in the glass transition temperature, and in the refractive index was observed. From the Raman and IR spectra studied the evidence is given for the phosphate network depolymerization as PbO content increases. Increase in PbO content leads also to an increase in refractive index (n) up to $n = 1.74$, for $x = 55$, and to an increase in the glass transition temperature (T_g) from $T_g = 270$ °C ($x = 30$) to $T_g = 360$ °C ($x = 55$).

Introduction

Phosphate glasses containing heavy metal oxide (HMO = PbO, Ga_2O_3, WO_3, etc.) were studied in a number of papers [1–15]. Attention was given to the systems where the most typical physical properties of phosphate glasses e.g., low glass-transition temperature 280–380 °C [2], rather high thermal expansion coefficient, the high UV transmission and high refractive index, are conserved [1–6 and papers cited therein]. Suitably modified phosphate glasses acquire also good chemical stability for practical applications, e.g., for nuclear waste hosts and storage [7], high power laser applications [7, 8], some sealing applications [9], non-linear optical devices [10] etc.

In the last years a various properties of $PbO–ZnO–P_2O_5$ glasses were studied in [1–3, 5, 10–13]. The main attention was given to the glasses with the formal molar content of P_2O_5 around 50%.

In this communication we summarize our results related to the density, the glass-transition temperature, the refractive index and to both the infrared and Raman spectra of the series $10ZnO–xPbO–(90–x)\ P_2O_5$ glasses. Glasses under study cover a wide compositional range from ultraphosphate ($[P_2O_5] > 50$ mol%) up to polyphosphate compositions ($[P_2O_5] < 50$ mol%).

Experimental techniques

Glass preparation

The glasses with general formula $10ZnO–xPbO–(90–x)\ P_2O_5$, $30 \le x$ (mol%) ≤ 55, were prepared in batches of 20 g from oxides PbO, ZnO (purity >97%, Aldrich), and H_3PO_4 (85%, p.a., Lachema, CZ) in Pt-crucible. The chemical composition of the glasses prepared is listed in the Table 1. The stoichiometric amounts of oxides and H_3PO_4 (diluted by distilled water) were mixed in Pt crucible and slowly heated (approximately 3 h), in an electrical furnace from the room temperature up to ~500 °C. At this temperature the crucible was annealed for about 3 h. In the next step the Pt crucible with the mixture of oxides was inserted into

H. Tichá (✉) · J. Schwarz
Faculty of Chemical Technology, University of Pardubice, 53210 Pardubice, Czech Republic
e-mail: Helena.Ticha@upce.cz

L. Tichý
Joint Laboratory of Solid State Chemistry, Institute of Macromolecular Chemistry, Academy of Sciences of the Czech Republic, University of Pardubice, Pardubice 53210, Czech Republic

Table 1 Sample number (No), the chemical composition (in mol%), the molar weight (M), the dilatometric glass transition temperature (T_g), the hydrostatic density ($\rho\rho$), the molar volume (V_m), and the values of the refractive index (n) for the spectral region 600–800 nm (refractive index dispersion is neglected) of studied glasses

No	Chem. composition			M [g/mol]	T_g [°C]	ρ [g/cm^3]	V_m [cm^3/mol]	n
	PbO	ZnO	P_2O_5					
1	30	10	60	160.3	270	3.74	42.81	1.58
2	35	10	55	164.3	273	3.99	41.18	1.57
3	40	10	50	168.4	320	4.31	39.10	1.66
4	45	10	45	172.5	325	4.68	36.87	1.67
5	50	10	40	176.5	344	5.10	34.77	1.73
6	55	10	35	180.6	359	5.50	32.82	1.74

another preheated electrical furnace ($T \approx 1{,}050$ °C) and after approximately 20 min of the melt-annealing at this temperature, the melt was poured onto a stainless plate. Glassy (confirmed by XRD analysis), colourless and well transparent samples were obtained. Glasses prepared were stored in desiccator filled with dry argon to preclude the hydrolysis mainly of ultraphosphate glasses. The chemical composition of the glasses prepared was verified using microprobe X-ray analysis (JEOL JSM 5500 LV) with a precision ±1.5% in atomic fraction of elements.

Glass characterization

The density (ρ) of the glasses studied was determined on the bulk samples by the standard Archimedean method using CCl_4 as immersion liquid. From the experimental values of the density, the values of molar volume (V_m) were calculated using the expression $V_m = M/\rho$, where M is the average molar weight of the glass.

The values of the dilatometric glass-transition temperature (T_g) were estimated by thermomechanical analysis. The cube ($5 \times 5 \times 5$ mm) of a glass was heated (the heating rate of 5 K min^{-1}, load $\approx$ 10 mN, equipment TMA CX04 (R.M.I., Czech Republic)) and from the ''low'' and ''high'' temperature parts of expansion curve the T_g value was determined using the slope intercept method.

The values of refractive index were estimated as geometric average $n = (n^2_R\, n_T)^{1/3}$, where $n_R = (1 + R^{1/2})/(1–R^{1/2})$, $n_T = [1 + (1–T^2)^{1/2}]/T$, T is transmittivity and R is reflectivity of the sample at the wavelength $\lambda = 800$ nm, i.e., in the transparent region of glasses studied [16]. Infrared spectra were recorded at room temperature on the Nicolet Nexus spectrophotometer in the specular reflectance mode, spectral region 400 < ν [cm^{-1}] < 1,500. Thick samples (the thickness $d \geq 0.4$ cm) with naturally reflecting surface were used for measurements; the backside of the samples was always mechanically roughened and darkened by a black absorbing paste to minimize any back reflection. The reflectance data were analyzed by the Kramers-Kronig inversion technique and the absorbance spectrum using the software supplied by Nicolet was obtained. Because of a presence of an atmospheric humidity that can affect the reflectance spectra especially of ultraphosphate glasses, these ones were taken from the just polished glasses. For a rough check of water presence in some glasses the transmission spectra in the mid-infrared region were measured on the both side optically polished planparallel plates ($d \sim 0.3$ cm, Nicolet Nexus spectrophotometer).

Raman spectra were recorded on an FTIR spectrometer, Bruker model IFS 55 with Raman attachment FRA 106, under excitation with a Nd:YAG laser radiation (excitation light wavelength 1,064 nm, a slit width of 4 cm^{-1}, the laser power ≈300 mW) at the sample surface. Raman spectra were measured at room temperature in the spectral region 50–1,500 cm^{-1}, using 200 scans on the bulk sample Nos. 3–6, and using 50 scans in the case of glasses No. 1 and 2, respectively.

Results and discussion

Chemical composition of glasses prepared, the molar weight (M), the glass transition temperature (T_g), the density (ρ), the values of molar volume (V_m), and the refractive index (n) values, are summarized in the Table 1.

For reader's convenience the variation of V_m, T_g and n values with increasing PbO content and corresponding decrease in P_2O_5 content, is shown in Fig. 1. The molar volume decreases with increasing PbO content nearly monotonously, which we ascribe to ''shrinkage'' of the starting phosphate network associated also by the substitution of phosphate tetrahedra by more efficiently packed Pb based polyhedra.

Contrary to $V_m(x)$ dependence both the $T_g(x)$ and $n(x)$ dependencies are non-monotonous indicating possible structural changes in the phosphate network of glasses studied. For example, for glasses with $x = 30$, 35 (ultraphosphates) the value of T_g remains to be nearly unchanged ($T_g \sim 270$–273 °C). With further increase in PbO content the abrupt increase in T_g by nearly 40 °C for $x = 40$ (metaphosphate composition) and by nearly 90 °C for $x = 50$, 55 (polyphosphates), indicates some progressive modification of the structure in this concentration region. Observed increase in

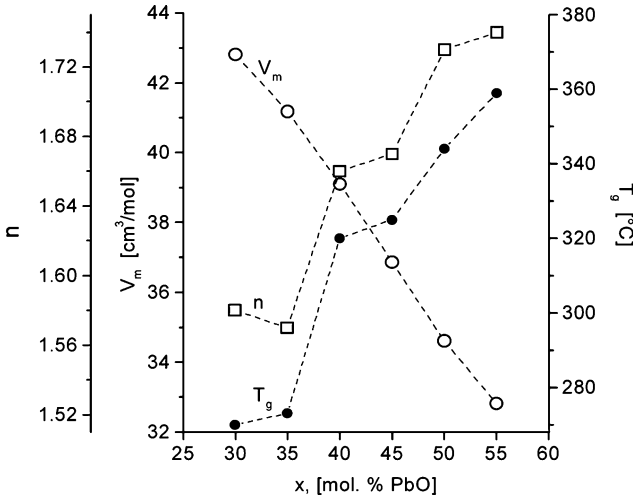

Fig. 1 The variation of the molar volume (V_m, marked by ○), the refractive index (n, marked by □), and the glass-transition temperature (T_g, marked by ●) with increasing content of PbO in glasses studied, see also Table 1. The experimental error bars are for V_m: ±0.5% V_m, for T_g: ±1.1% T_g , for n: ±2.0% n, respectively. The dashed lines are only the guides for the eye

T_g could be associated also with a decrease in content of some residual water. Indeed in the infrared transmission spectra of the samples where $x = 30$–45 we observed (i) rather broad and weak feature in the region 2,700–3,000 cm^{-1} which indicates a presence of some interior hydroxyl groups (P–OH), and (ii) a weak feature at around 3,600 cm^{-1} indicating absorbed water [17]. The intensity of the last feature, namely for glasses where $x = 30$ and 35, respectively, increases if unprotected sample is exposed to the atmospheric humidity. We, however, suppose that the main origin of an increase in T_g cannot be associated to a decrease in the content of residual water. The feature seen in the region 2,700–3,000 cm^{-1} we observed for chemical compositions where $x = 30$–45 is weak and broad indicating rather low content of interior hydroxyl groups. However, in the same concentration PbO content ($35 \le x \le 40$) a step-like increase in T_g is evident (Fig. 1). Hence, we suppose that the main origin of an increase in T_g cannot be attributed only to a reduction in residual water in glassy network but it is mainly associated with some other structural changes.

In the pure vitreous P_2O_5 and glassy ultraphosphates with the high content of P_2O_5, the basic structural entities are the PO_4 tetrahedra forming predominantly 3-dimensional network (3D-network, Q^3 type of structural units[1].) [18]. For reasonably low content of a modifier a part of 3D-network can depolymerise and 2D-chain structure is simultaneously formed (Q^2 structural unit[2].) According to Brow [19], in the ultraphosphate region of binary phosphate systems, the fraction of Q^2 and Q^3 units can be calculated by relations: $f(Q^2) = x/(1–x)$; $f(Q^3) = (1–2x)/(1–x)$, where x means the content of the second oxide in a glass. Assuming that in the ultraphosphate region of studied glasses, $x \le 35$, both the PbO and ZnO have mainly a modifying effect in the phosphate network we calculate $f(Q^2) = 0.67$, $f(Q^3) = 0.33$ for the composition $10ZnO–30PbO–60P_2O_5$, and $f(Q^2) = 0.818$, $f(Q^3) = 0.182$ for the composition $10ZnO–35PbO–55P_2O_5$. That is with increasing content of PbO, the fraction of 3D-network structure decreases quickly and the chain structure created by Q^2 units dominates to the network. Hence, rather low values of T_g observed in the region where $x \le 35$ mol% PbO are supposed to be due to the network structure formed by ($Q^3 + Q^2$) structural units.

For PbO content $x \ge 35$ some chains can be cross-linked by formation of few covalent Pb–O–P linkages. We notice that a small content of ZnO (<15 mol%) has mainly modifying effect on the glass properties [20, 21]. Hence, as PbO content increases the amount of linkages Pb–O–P also increases. The chains (Q^2 units) are more cross-linked, the network structure is more stabilized by Pb–O–P linkages, and T_g increases. This one is documented in Fig. 1 where a rise in T_g up to ~360 °C for chemical composition with $x = 55$ mol% PbO, is evident. The $n(x)$ dependence is also rather non-monotonous and three regions are evident there, see Fig. 1. We suppose for chemical compositions where $x > 35$ that all features observed, i.e., the increase in the density, the structural changes associated with an increase in the cross-linking by Pb–O–P linkages and also an increase in the overall polarizability namely due to an increase in PbO content are responsible for the step like increase in the refractive index values. As stressed in [22] polarizability of Zn^{2+} and Pb^{2+} cations assist them to interact with terminal oxygen atoms of improperly oriented PO_4 groups. In such a case, from the point of view of medium range order, both cations can behave like network formers.

Raman (R) and infrared reflectivity (IR) spectra of glasses studied well correspond to R and IR spectra of typical Pb- and Zn- phosphate glasses [1–5, 11]. In Raman spectra of glasses studied (Fig. 2) starting from the composition with 30 mol% of lead oxide, it is seen:

[1] Q^3 is PO_4 tetrahedron with three bridging and one non-bridging oxygen [18].

[2] Q^2 is PO_4 tetrahedron with two bridging and two non-bridging oxygens (metaphosphate unit) [18].

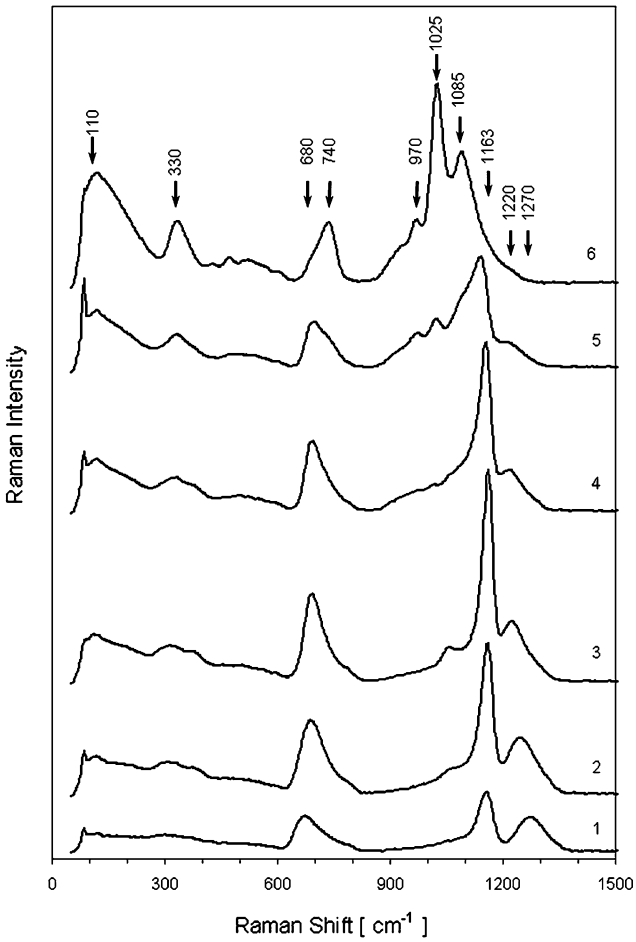

Fig. 2 Raman spectra of glasses studied. The numbers indicate the chemical composition of the glasses studied, see Table 1

(i) The middle to low intensity band at $v \sim 1{,}270$ cm^{-1} is moving to lower frequencies (the trend is: $v \sim 1{,}270$ ($x = 30$) $\rightarrow$ 1,240 ($x = 35$) $\rightarrow$ 1,220 ($x = 40$–50) cm^{-1}, respectively [1, 6, 19]. Generally, this band is the asymmetric PO_2 stretch mode (ν_{as} (PO_2) [1, 2, 6] but in the case of ultraphosphate compositions one cannot exclude the contribution of the stretching of Q^3—type of tetrahedra. These bands are undistinguishable in the case of ultraphosphate compositions (glass No. 1 in our case).

(ii) The main band at ~1,163 cm^{-1} is due the symmetric stretching of bridging oxygens in Q^2 tetrahedra ($\nu_s(PO_2)$, [19]) and its position remains unchanged up to $x \sim 45$ mol% PbO. Further addition of PbO up to 55 mol% results in the moving of the band towards lower frequencies (the trend is: $v \sim 1{,}163(x = 30$–45, resp.) $\rightarrow$ $1{,}100(x = 50)$ $\rightarrow$ 1,085 and $1{,}025(x = 55)$ cm^{-1}, resp.).

(iii) The band at $v \sim 680$–740 cm^{-1}, its intensity/area increases up to $x \sim 45$ mol% PbO and for $x > 45$ its intensity decreases. This one is assigned to symmetric stretching of bridging oxygens ((ν_s (POP)) connecting the neighboring PO_4 tetrahedra in Q^2 chains [1–3, 19]. For the glass with $x = 55$ ($10ZnO$–$55PbO$–$35P_2O_5$) the Raman spectrum is characterized by the band at $v \sim 1{,}025$ cm^{-1} (the main band), by the other strong band at $v \sim 1{,}085$ cm^{-1}, and by a new well resolved band at $v \sim 970$ cm^{-1} (Fig. 2). The glass structure is formed mainly by the chains of diphosphates ($v \sim 1{,}025$ cm^{-1}), tri- and tetra-phosphates ($v \sim 1{,}085$ cm^{-1}). The band at around 970 cm^{-1} corresponds to vibrations of PO_3-end groups in these polyphosphates (Q^1 structural unit[3].) [1–3].

(iv) In the low frequency region ($v < 400$ cm^{-1}), with increasing content of PbO, the new bands around $v \sim 330$ cm^{-1} and $v \sim 110$ cm^{-1}, appear. According [4, 5] the band ~330 cm^{-1} is due to an overlap of both the bond-bending vibrations in phosphate chains and the vibration of Pb–O covalent bond in tetragonal pyramids. We suppose that the origin of this band can be attributed mainly to PbO. As shown in [23] both the tetragonal and orthorhombic PbO modifications have in the region 300–400 cm^{-1} peaks at $v \sim 337$ cm^{-1} (tetragonal PbO) and at $v \sim 345$ cm^{-1} (orthorhombic PbO). Moreover, for orthorhombic PbO the typical Raman band at $v \sim 290$ cm^{-1} exists there but that one is fully absent in Raman spectra of tetragonal PbO [23]. In Raman spectra of glasses studied there is no indication of the presence of such Raman band, namely in glasses with high content of PbO as documented in Fig. 2, curves 5 and 6. Consequently, we suppose that Raman band at ~330 cm^{-1}, we observed, is associated with the presence of tetragonal PbO. The broad and asymmetric low frequency Raman band at ~110 cm^{-1} varies in the shape and intensity with PbO content. We suppose that this Raman feature consists not only from the most intense mode of tetragonal PbO at $v \sim 143$ cm^{-1} [23] but broadening of its indicates also various lead–oxygen vibrations originating from a presence of entities based for instance on $Pb_3P_4O_{13}$ and $Pb_2P_2O_7$ as suggested for another composition series in PbO–ZnO–P_2O_5 glasses [5].

Infrared spectra (IR) of glasses studied (Fig. 3) confirm the results obtained by Raman spectroscopy. With increasing content of PbO it is seen in Fig. 3:

[3] Q^1 is PO_4 tetrahedron with one bridging and three non-bridging oxygens (PO_3-end group) [18].

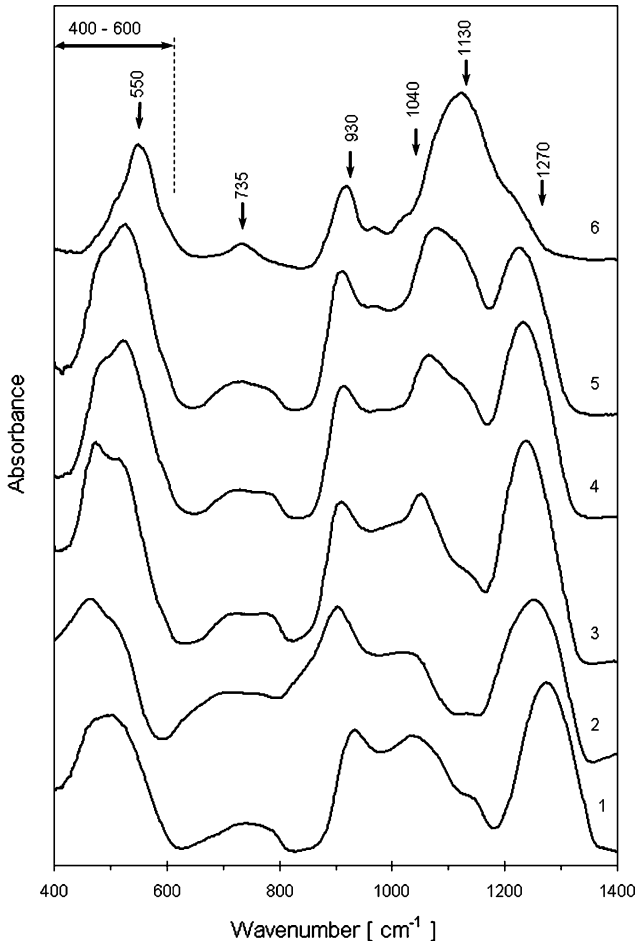

Fig. 3 Infrared spectra of glasses studied. The numbers indicate the chemical composition of the glasses studied, see Table 1

(i) The band at ~1,270 cm^{-1}, attributed to the absorption of P=O in Q^3 unit and $(PO_2)_{as}$ in Q^2 chains [24] is moving steeply to lower frequency (up to ~1,120 cm^{-1}) indicating that the long Q^2 chains are dominant, especially when the content of PbO <45 mol%. The intensity of this band decreases very quickly, the amount of long chains is reduced, and thus the structure of phosphate glasses is composed from shorter chains (Q^1), and/or isolated tetrahedra (Q^0 structural unit[4].).

(ii) The absorption band at ~1,040 cm^{-1} is moving up to v ~ 1,130 cm^{-1}, and its progression supports the idea of fragmentation of structure with substitution of P_2O_5 by PbO probably with an assistance of ZnO. In [11 and papers cited therein] this band is attributed to the absorption due to Pb–O–P or Zn–O–P in-between neighboring chains linkages.

(iii) The absorption band at v ~ 930 cm^{-1} is slightly moving to v ~ 905 cm^{-1}, and it is attributed to asymmetric stretching vibrations of P–O–P groups [11]. Intensity of this band decreases as PbO content increases.

(iv) The broad envelope in the region v ~ (650–830) cm^{-1} becomes narrower and for the last composition studied it is centered at v ~ 735 cm^{-1}. It is ascribed to the stretching vibration of oxygen atoms in P–O–P bridges [19]. Its centering indicates increasing number of Q^1 units.

(v) In the region of v ~ 400–600 cm^{-1}, starting from ultraphosphate composition, relatively intensive absorption band, rather an envelope of at least two bands, is seen. As PbO content increases, the shape and position of this band is changing. Finally, for $x = 55$ the dominant component of this band evident at v ~ 550 cm^{-1} can be ascribed to bending vibrations of P–O bonds of basic structural units of phosphate glasses [19].

Both the IR spectra and Raman spectra imply mainly considerable fragmentation/depolymerization of the phosphate network with an increase of PbO content in the glass network. This is in harmony with [25] where it is concluded that...''the PO_4 network depolymerization is the dominating principle in phosphate glasses''. We suppose that in studied glasses lead oxide as a glass modifier enters the glass by breaking up the P–O–P bonds, and perhaps introduces coordinate defects along with non-bridging oxygen ions. At higher content PbO ($x > 35$), however, can also participate in the glass network formation. By creating the PbO_4 tetragonal pyramids with Pb(II) in the apex (Raman band at ~330 cm^{-1}). In this case Pb(II) connects the phosphate tetrahedra by Pb–O–P linkages which results in cross linking increase. In fact this is the case when due to an increase in the concentration of modifier cations the probability that two terminal oxygen atoms of PO_4 group can interact with different M^{n+} sites increases [25] and such cation behaves like network former. Hence, the glass-transition temperature increases even in the case of the phosphate network fragmentation.

Conclusion

In the present communication the density, the molar volume, the glass transition temperature, the refractive index, infrared and Raman spectra of glasses $10ZnO–xPbO–(90–x)P_2O_5$, where $30 \le x$ (mol% PbO) ≤ 55, were examined. With an increase in PbO content the

[4] Q^0 is PO_4 tetrahedron with four non-bridging oxygens [18].

values of density increase from 3.74 g/cm^3 (x = 35) up to 5.5 g/cm^3 (x = 55). The values of the refractive index (n) were found in the region 1.58 (x = 35) < n < 1.74 (x = 55) and the values of the glass-transition temperature (T_g, [°C]) were found in the region 270 (x = 35) < T_g < 359 (x = 55). Infrared and Raman spectra reveal the fragmentation of the ultraphosphate network associated also with P–O–Pb linkages formation as PbO content increases. These linkages are suggested to be responsible for cross-linking between chains formed by Q^2 units. Consequently, the glass transition temperature increases as PbO content increases. We suppose that in glasses with higher content of PbO (x > 40), the simultaneous presence of Raman bands at ~110 and at ~330 cm^{-1}, resp., indicate that PbO is mainly incorporated into a glassy matrix as tetragonal pyramids and behaves rather as the network former.

Acknowledgements This work was supported by the project MSM 0021627501 of the Czech Ministry of Education and by GACR project 340711/51. L.T. acknowledges also support from the project AVOZ 40500505. We also acknowledge to M.Vlček[a] and M.Kincl[b] for kind measurements of the Raman and infrared spectra, respectively.

References

1. Liu HS, Chin TS (1997) Phys Chem Glasses 38(3):123
2. Liu HS, Chin TS, Yung SW (1997) Mater Chem Phys 50:1
3. Liu HS, Shih PY, Chin TS (1996) Phys Chem Glasses 37:227
4. Subbalakshmi P, Veeraiah N (2002) Mater Lett 56:880
5. Saout GL, Fayon F, Bessada C, Simon P, Blion A, Vaills Y (2001) J Non-Cryst Solids 293/295:657
6. Brow RK (1997) J Non Cryst Solids 222:396
7. Day DE, Wu Z, Ray CS, Hrma P (1998) J Non-Cryst Solids 241:1
8. Weber MJ (1990) J Non Cryst Solids 123:208
9. Brow RK, Kovacic L, Loehman RE (1996) Ceram Trans 70:177
10. Schwarz J, Tichá H (2003) Sci Pap Univ Pardubice A 9:79
11. Young SW, Shioh PY, Chin TS (1998) Mater Chem Phys 57:111
12. Meyer K (1997) J Non Cryst Solids 209:227
13. Martin SW (1991) Eur J Solid State Inorg Chem 28:163
14. Subbalakshmi P, Veeraiah N (2002) J Non-Cryst Solids 298:381
15. Qi YF, He L (1986) J Non-Cryst Solids 80:527
16. Schwarz J, Tichá H (2002) J Opt Adv Mater 4:381
17. Abe Y, Hosono H, Ohta Y, Hench LL (1988) Phys. Rev B 38:10166
18. Van Wazer JR (1958) Phosphorus and its compounds, vol. 1. Interscience, New York
19. Brow RK (2000) J Non Cryst Solids 263&264:1; ibid (1995) 191:45
20. Montagne L, Palavit G, Delaval R (1998) J Non Cryst Solids 223:43
21. Sales BC, Otaigbe JU, Belal GH, Boatner LA, Ramey JO (1998) J Non Cryst Solids 226:287
22. Hoppe U, Walter G, Kranold R, Stachel D (2000) J Non Cryst Solids 263&264:29
23. Wiechert DU, Grabowski SP, Simon M (2005) Thin Solids Films 484:73
24. Gresch R, Mueller-Wartmuth W, Dutz H (1979) J Non Cryst Solids 34:127
25. Hoppe U (1996) J Non Cryst Solids 195:138